MALDI mass spectrometry imaging in rheumatic diseases

Biochimica et Biophysica Acta 1865 (2017) 784–794

Contents lists available at ScienceDirect

Biochimica et Biophysica Acta

journal homepage: www.elsevier.com/locate/bbapap

Review

MALDI mass spectrometry imaging in rheumatic diseases☆

Beatriz Rocha [a], Berta Cillero-Pastor [b], Francisco J. Blanco [a,c,*], Cristina Ruiz-Romero [a,d,*]

[a] Proteomics Unit-ProteoRed/ISCIII, Rheumatology Group, INIBIC – Hospital Universitario de A Coruña, SERGAS, A Coruña, Spain
[b] Imaging Mass Spectrometry (IMS), M4I, Maastricht University, The Netherlands
[c] RIER-RED de Inflamación y Enfermedades Reumáticas, INIBIC-CHUAC, A Coruña, Spain
[d] CIBER-BBN Instituto de Salud Carlos III, INIBIC-CHUAC, A Coruña, Spain

ARTICLE INFO

Article history:
Received 2 July 2016
Received in revised form 29 September 2016
Accepted 4 October 2016
Available online 11 October 2016

Keywords:
MALDI-MSI
Rheumatic diseases
Osteoarthritis
Rheumatoid arthritis
Synovium
Cartilage

ABSTRACT

Mass spectrometry imaging (MSI) is a technique used to visualize the spatial distribution of biomolecules such as peptides, proteins, lipids or other organic compounds by their molecular masses. Among the different MSI strategies, MALDI-MSI provides a sensitive and label-free approach for imaging of a wide variety of protein or peptide biomarkers from the surface of tissue sections, being currently used in an increasing number of biomedical applications such as biomarker discovery and tissue classification. In the field of rheumatology, MALDI-MSI has been applied to date for the analysis of joint tissues such as synovial membrane or cartilage. This review summarizes the studies and key achievements obtained using MALDI-MSI to increase understanding on rheumatic pathologies and to describe potential diagnostic or prognostic biomarkers of these diseases. This article is part of a Special Issue entitled: MALDI Imaging, edited by Dr. Corinna Henkel and Prof. Peter Hoffmann.

1. Introduction

Mass spectrometry imaging (MSI) is an analytical technique employed for determining both the relative abundance and the spatial distribution of biomolecules in tissue sections without using any labeling or staining [1]. These biomolecules can be lipids, peptides, proteins, metabolites and even elemental ions [2–4]. The main advantage of MSI is the possibility to study different areas of a tissue section with or without previous knowledge of the heterogeneity of the sample [5]. Therefore, MSI has already shown its usefulness for a number of applications, including biomarker discovery, tissue/patient classification or drug monitoring. Among the different MSI strategies, MALDI-MSI has been used in an increasing number of biomedical applications such as biomarker discovery and tissue classification. In the present review, we present an overview of those recent studies carried out in the rheumatology field using MALDI-MSI. These include analyses of tissues from affected joints, such as osteoarthritic cartilage and synovium, meniscal lesions, osteoporotic bone or synovium from rheumatoid arthritis or haemophilic arthritis patients. Furthermore, we describe the application of other MSI techniques, such as secondary ion mass spectrometry (SIMS), for the characterization of these tissues and also to analyze the early steps of the chondrogenic process induced in mesenchymal stem cells.

2. MSI workflow for protein and peptide analysis in joint-derived samples

MALDI-MSI is a multi-step process involving sample preparation, data acquisition, processing and visualization. A typical workflow summarizing the general process for the detection of tryptic peptides in cartilage samples by MALDI-MSI is described in Fig. 1. This workflow requires an antigen retrieval step following deparaffinization for FFPE samples, in situ trypsin digestion, matrix application and MSI acquisition. Briefly, sample surface is treated with a proteolytic enzyme, such as trypsin, in order to detect proteins above 25 kDa. After digestion, samples are covered with a suitable matrix solution and introduced in the mass spectrometer. Then, the tryptic peptides are desorbed from the tissue surface

Abbreviations: ACN, Acetonitrile; CHCA, α-cyano-4-hydroxycinnamic acid; CMC, Carboxymethyl cellulose; COMP, Cartilage oligomeric matrix protein; DESI, Desorption electrospray ionization; DHB, Dihydroxybenzoic acid; 2,4-DNPH, 2,4 dinitrophenylhydrazine; ECM, Extracellular matrix; ESI, Electrospray ionization; FA, Fatty acids; FFPE, Formaldehyde fixed and paraffin embedded; FM, Fibromodulin; FN, Fibronectin; HA, Haemophilic arthropathy; HAp, Hidroxyapatite; IHC, Immunohistochemistry; ITO, Indium tin oxide; LAESI, Laser ablation electrospray ionization; LESA, Liquid extraction surface analysis; LC, Liquid chromatography; MALDI, Matrix-assisted laser desorption/ionization; MS, Mass spectrometry; MS/MS, Tandem mass spectrometry; MSCs, Mesenchymal stem cells; MSI, Mass spectrometry imaging; Mw, Molecular weight; OA, Osteoarthritis; PC, Phosphatidylcholine; PE, Phosphatidylethanolamine; PG, Phosphatidylglycerol; PI, Phosphatidylinositol; Nano-DESI, Nanospray desorption electrospray ionization; NIMS, Nanostructure-initiator mass spectrometry; RA, Rheumatoid arthritis; ROI, Region of interest; SIMS, Secondary ion mass spectrometry; SM, Sphingomyelin; ST, Sulfatide; TFA, Trifluoroacetic acid; TOF, Time of flight.

☆ This article is part of a Special Issue entitled: MALDI Imaging, edited by Dr. Corinna Henkel and Prof. Peter Hoffmann.

* Corresponding authors at: Rheumatology Division, Instituto de Investigación Biomédica de A Coruña (INIBIC), As Xubias, 84, 15006 A Coruña, Spain.
E-mail addresses: fblagar@sergas.es (F.J. Blanco), cristina.ruiz.romero@sergas.es (C. Ruiz-Romero).

http://dx.doi.org/10.1016/j.bbapap.2016.10.004
1570-9639/

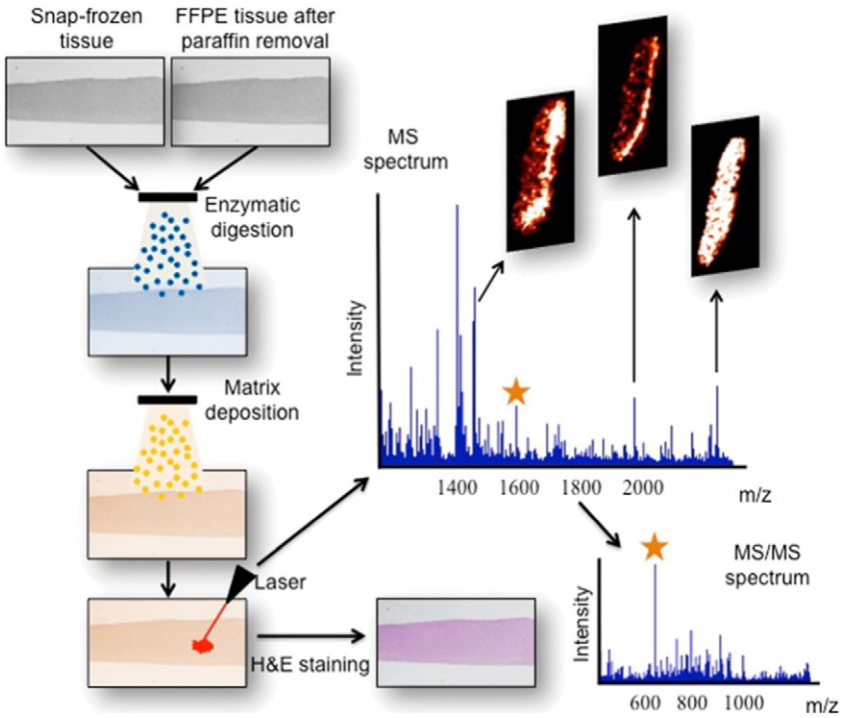

Fig. 1. Representative workflow for protein identification in cartilage samples by MALDI-MSI. Cartilage tissue (either snap-frozen or FFPE) is cut in thin slices and collected on conductive plates. FFPE sections should be previously deparaffinized and antigen retrieved. Then, trypsin solution followed by matrix solution is usually automatically spotted onto the section. Mass spectra are acquired from many points of the tissue section and subjected to statistical analysis to select candidates for suitable identification. Bidimensional ion images are finally reconstructed from the mass spectra, indicating the spatial distribution of the detected tryptic peptides. Target tryptic peptides are then identified by MS/MS. Subsequent to the MALDI measurement, sections may also be stained for histological analyses.

using a matrix-assisted laser desorption/ionization (MALDI) source. After MALDI-MSI analysis, the corresponding mass spectral data is analyzed by statistical tools in order to select the peptide precursors of interest. MALDI-MS/MS experiments can be directly performed over the tissue to obtain sequence information for the tryptic peptides and thereby identify the original protein. In addition, peptides can be also extracted from the tissue samples and analyzed by LC-MS/MS for protein identification. Finally, MSI data can be correlated with different histological areas using classical staining like hematoxylin and eosin.

2.1. Sample preparation of joint-derived tissues

MSI is commonly performed over fresh frozen tissues. Cartilage, synovial membrane and meniscus tissue can be taken from the knee and snap frozen in liquid nitrogen within hours. An alternative method is to fix the samples immediately in formalin after collection and embed in paraffin. However, formalin-fixed paraffin-embedded (FFPE) tissues require additional sample preparation steps to reverse protein cross-linking and remove paraffin, which is incompatible with MS [6,7]. For fragile or small tissues, like cellular pellets, it is possible to embed the samples in gelatin in order to facilitate the cutting process. Methacrylate-based resins are commonly used as embedding materials for mineralized hard tissues like bone. All tissues biopsies, organs, or whole organisms should be immediately stabilized after collection to preserve tissue morphology and avoid spatial delocalization and degradation of the proteins through endogenous enzymes or oxidation processes. Some specific devices, which combine heat and pressure, have been developed in order to stop the degradation activity [8,9]. Sample stabilization step can be performed before or after freezing the samples. Frozen tissues are usually cut at 10–12 μm, whereas FFPE samples are approximately cut between 3–4 μm [10]. Tissues slides are then mounted onto regular glass slides, metal targets or metal-coated glass slides (indium tin oxide (ITO)-coated slides) depending on the mass spectrometer [11,12]. Consecutive tissue sections can be stained in order to correlate MSI and histology images, which can be performed either before or after an MSI experiment. If staining is carried out before MSI measurements, the sections must be stained with histological stains compatible with MSI, like methylene blue or cresyl violet [13]. After MSI analysis, sections can be also stained with hematoxylin and eosin after matrix removal [14,15].

Tissue samples can be then washed to remove ionization-suppressing small molecules, salts or lipids in order to increase the efficiency of the enzymatic digestion and the detection of the tryptic peptides [16]. The most commonly employed washing protocol involves ethyl alcohol washes at different percentages [7,17]. Other solvents such as acetic acid, chloroform or toluene have been successfully applied to eliminate salts and lipids in frozen tissues. Snap frozen cartilage and synovial membrane are usually rinsed in 100% ethyl alcohol for 30 s and 2 min in 70% ethyl alcohol. A final washing step in chloroform for 30 s is optional [18–20]. For FFPE tissues, deparaffination is a crucial step that involves washing the samples in toluene or xylene and then rehydrating in a graded ethanol series before drying at room temperature [6,7]. FFPE synovial tissues are largely deparaffined in xylene (100% twice for 3 min), and then rehydrated with successive washes in 95% and 70% ethyl alcohol for 1 min each [21]. Protein cross-linking induced by formalin fixation can be reduced using either enzymatic or heat-mediated processes [22,23]. The most common protocol uses a heating step because it denatures the proteins allowing a more efficient proteolysis. In addition, recent methods have incorporated the use of high temperature citric acid buffering to allow partial reversal of FFPE protein cross-linking [24]. Antigen-retrieval of FFPE synovial membrane can be performed incubating the slides in Tris-HCl buffer at pH 9.0, at 95 °C for 20 min. All these washing steps can be performed using different methods. The use of a beaker and pipetting are the two frequent solvent application methods used for FFPE samples. A recent alternative to this standard washing that is applicable to frozen delicate tissues uses paper blotting of sample. This procedure uses solvent wetted fiber-free paper to enable local washing of tissue sections for MALDI-MSI and tissue profiling experiments [25]. In recent years, the processes of

deparaffinization and antigen retrieval for MALDI-MSI analysis of FFPE tissues have been optimized [26–29]. These protocols suggest that samples should be heated for 1 h at 60 °C and directly transferred into xylene solution (100%, twice for 2–5 min), ethanol (70%, twice 2–3 min) and HPLC grade H_2O or NH_4HCO_3 buffer (10 mM, twice for 3 min) for deparaffinization. Heat-induced antigen retrieval in the presence of citric acid solution (98 °C, 30 min) has been proposed as the best option. After antigen retrieval step, samples should be cooled down in NH_4HCO_3 buffer (10 mM, twice for 1 min) to optimize the pH for the following on-tissue digestion. Apart from this optimized protocol, alternative methods have been found suitable for both lipids and peptide imaging. For instance, it has been described that tissue samples fixed with formalin and processed without the paraffin embedding step provide results of protein/peptide imaging comparable to those obtained for classical FFPE and fresh-frozen samples [27].

The next step of sample preparation in a MALDI-MSI experiment (as shown in Fig. 1) is the application of the proteolytic enzyme on the tissue or region of interest (ROI). The digestion of the tissue produces characteristic peptides that will allow us to locate and identify the corresponding proteins. Different parameters, including the buffer used, the concentration of the enzyme or the time and temperature of incubation must be optimized according to the analyzed sample. Among the different enzymes, trypsin is the most commonly employed enzyme in the imaging field. Several detergents, such as octylglucoside, or surfactants, like RapiGest (Waters), can be added before trypsin application to improve the efficiency of trypsin activity and thereby enhance the detection and identification of proteins [30]. Joint-derived tissues digestion is usually performed at temperatures ranging from RT to 37 °C for an incubation period of 1.5 h until several hours (e.g. overnight) depending on the research tissue and protocol used. For instance, cartilage samples are mainly incubated overnight at 37 °C with 50 ng/μl trypsin solution. The slides should be kept in a wet atmosphere in order to avoid the dehydration of the enzyme/tissue. Other enzymes like chymotrypsin, elastase, pepsin or PNGase F have been used in MALDI-MSI either alone or in combination with trypsin [31–33]. After digestion, samples are then covered with a matrix solution. Matrices are in general small organic compounds whose function is to promote the ionization of the molecules. Matrix deposition, as well as enzyme application, can be performed through spraying or spotting methods. Several different types of matrices are used for MALDI-MSI, which are usually determined by the type of molecules that are to be investigated. The most used matrix for peptide detection in joint derived tissues is α-cyano-4-hydroxycinnamic acid (CHCA) at 7–10 mg/ml and dissolved in different organic solvents like acetonitrile (ACN), ethanol or methanol with trifluoroacetic acid (TFA) (0.1 to 0.5%). 2,5-dihydroxybenzoic acid (DHB) has been also reported as a useful matrix for peptide identification in the mouse brain [34,35]. Sinapinic acid (3,5-dimethoxy-4-hydroxycinnamic acid, SA) is a matrix commonly used to map the spatial distribution of peptides and high Mw proteins [11,36,37]. Location of several proteins in the synovial sublining and lining layer has been easily achieved using SA at 20 mg/ml and dissolved in 1:1 ACN/0.2% TFA [38]. In addition, protein spatial distributions of prostate cancer tissue and skin have been recently obtained by MALDI-MSI employing SA as matrix [31, 39]. Several other matrices, such as aniline or 2,4 dinitrophenylhydrazine (2,4-DNPH) are also a good option for protein identification. It has been shown that the combination of 2,4-DNPH and CHCA is ideal for peptide extraction above 5000 kDa. Moreover, in FFPE samples, adducts corresponding to the formalin fixation are suppressed with this matrix [40].

2.2. Data acquisition

After sample preparation, the tissue sections are introduced in the mass spectrometer to perform the MS analysis. Firstly, the molecules within the tissue need to be ionized using a MALDI source. The ions generated by these approaches are then detected by their mass to charge ratio (m/z) in a mass analyzer, leading to a mass spectrum that shows the intensity of each detected ion. MALDI is often used for the analysis and detection of a wide range of molecular classes, mainly proteins and peptides, as well as small molecules such as lipids or metabolites [14]. Several matrices have been developed and optimized to analyze a wide variety of molecules by MALDI [41,42], although their use presents some limitations as they can interfere with the molecules from the sample and limit the resolution to the size of their crystals, which is typically many tens of microns. Table 1 shows an overview of those matrices that have been employed in this type of assays.

2.3. Data processing and visualization

MSI produces large data sets that contain a huge amount of information. The data are typically subjected to preprocessing steps prior to data analysis and ion image generation. The purpose of preprocessing is to remove artefacts introduced during the data acquisition, to make spectra comparable to one another and to improve the efficacy of peak detection [50]. The common preprocessing methods applied in MS are smoothing, baseline correction, realignment of the m/z scale, peak selection and matching, and normalization [51]. Normalization processes are performed in order to solve inherent limitations of the MALDI technique and sample preparation protocols, such as matrix heterogeneity and application, differential ionization efficiency, ion suppression due to sample complexity and composition, instrumental variation and differential levels of analyte solubility and extraction from different tissue regions [51–53]. Several different procedures are being used for MSI data normalization. Total Ion Current (TIC) is the most commonly normalization method used in practice in MSI field [53,54]. Here, the TIC (the sum of all intensities) is calculated for one spectrum and then all spectra intensities are divided by this TIC value [55]. Normalization can be also performed scaling the peak intensities by a factor calculated from matrix-related peaks. This type of normalization is mainly a correction for uneven matrix coating and is based on the fact that more analyte is measured if there is more matrix signal present, since the matrix co-crystallizes with the analytes. Apart from matrix signal, endogenous species with a homogenous tissue distribution can be used as reference molecules for data normalization. Recently, a method based on the median intensity of selected peaks has improved the normalization of MALDI-MSI data compared with the other procedures described above [56]. All these preprocessing steps can be performed automatically through different specialized software programs and tools included in the mass spectrometers, such as FlexImaging and ClinProTools (Bruker Daltonics, Bremen, Germany, www.bdal.com) [14], which can be used for data visualization and statistical analysis (multivariate analysis, classification, principal component analysis (PCA)); ImageQuest (ThermoFisher Scientific, Waltham, MA, USA), HDI software (Waters, Manchester, UK) which can be coupled to MaasLynx or Biomap (Novartis, Basel, Switzerland, www.maldi-msi.org) which can be also used for data visualization and calculating basic statistics of the full dataset or of ROI. Commercial SCiLS Lab (SCiLS, Bremen, Germany) is a very new software for visualization, analysis and interpretation of MALDI imaging data. Nowadays, in-house developments are necessary to increase the functionality and flexibility of commercial software and Matlab is probably the most popular platform for data analysis purpose in the MSI field. For instance, MSiReader is an open source software built on the Matlab environment to process, analyze and visualize imaging data [57]. Peptide localization in cartilage samples using Biomap software is illustrated in Fig. 2. Finally, mass spectra from multiple regions in the sections can be exported for subsequent statistical analysis such as principal component analysis (PCA) [58,59] or discriminant analysis (DA) [60]. PCA can be applied to the spectra from specific ROIs, in order to distinguish groups in the extracted spectra, and from the entire tissue section, to trace the distribution of the groups [50,61].

Table 1
Overview of the main matrices currently used for MALDI-MSI.

Matrix	Acronym	Application	Type	Reference
Alpha-cyano-4-hydroxycinnamic acid	CHCA	Small proteins, peptides and glycopeptides	Crystalline	[43]
3,5-dimethoxy-4-hydroxycinnamic acid	SA	Large proteins and peptides, lipids	Crystalline	[11,16,42]
2,5-dihidroxibenzoic acid	DHB	Sugars, proteins, peptides, nucleotides, phospholipids, drugs	Crystalline	[33,44]
2,6-dihidroxyacetphenone	DHA	Phospholipids, drugs	Crystalline	[16,42]
CHCA/aniline	–	Peptides	Solid ionic	[45]
CHCA/*N*,*N*-dimethylaniline	–	Peptides	Solid ionic	[45]
CHCA/2-amino-4-methyl-3-nitropyridine	–	Peptides	Liquid ionic	[45]
CHCA/n-butylamine	CHCAB	Peptides and lipids	Liquid ionic	[46]
2,4,6-trihydroxiacetophenone	THAP	Lipids and nucleotides	Crystalline	[47]
3-hydroxypicolinic acid	3-HPA	Glycoproteins, lipids and nucleotides	Crystalline	[41,42]
9-aminoacridine	9-AA	Phospholipids	Crystalline	[48]
4-paranitroaniline	PNA	Lipids	Crystalline	[49]

The combination of PCA with complementary statistical approaches, such as hierarchical clustering, is used to investigate if the real differences between groups are affected by inter-patient variability. In addition, the supervised method DA can be used after a preprocessing step with PCA. By these means, the PCA first reduces the dimensionality of the data (from several hundred MS peaks to a small number of principal components) obtaining different groups/conditions, and then the DA is calculated using the principal components to classify the predefined groups/conditions. This strategy has been successfully used to classify human cancer and cartilage samples based on protein profile patterns [18,62].

2.4. Identification and validation

Confident identification of the detected molecules can be achieved by tandem mass spectrometry (MS/MS) or accurate mass measurements, either on the same slide after performing the imaging analysis, or in a consecutive section. This allows correlation between the observed *m/z* and its identity. Peptide sequence information derived from MS/MS analysis provides the basis for protein identification. Tandem MS/MS provides amino acid sequence information on peptide fragments from a specific peptide. A peptide with good fragmentation spectra (minimum 6–7 aminoacids, and 4 consecutive amino acid ion series) or more than two peptides with minimal quality spectra are generally required for correct protein identification. MS/MS spectra are submitted into a database search engine to match tryptic peptide sequences to their respective intact proteins. One of the most used search engines is Mascot (www.matrixscience.com), which compares the experimental mass values with calculated peptide mass or fragment ion mass values, obtained by applying cleavage rules to the entries in a comprehensive primary sequence database. The sequence databases that can be searched on the Mascot server are MSDB, NCBInr, SwissProt, and dbEST [63]. Furthermore, there are other MSI databases available for protein identification. Some examples of public libraries of MALDI-MSI include MSiMass list database [64] and MaTisse [65]. In the last few years, several databases have become available, making the identification of lipids and metabolites much easier. Currently, the most employed lipidome databases include LipidBank [66,67], Lipid Maps [68,69], the Human Metabolome Database (HMBD) [70], and LipidBlast [71]. In the field of cell metabolites, databases such as METLIN [72], KEGG [73] and HMBD can be used.

Direct MS/MS measurements have the advantage of fast acquisition times and smaller data files. This method is very useful when high-resolution images are not needed. However, not all the precursor peaks (especially those corresponding to low abundant proteins) can be selected and fragmented using this approach. In fact, no more than a few tens of peptides are directly identified on tissue by tandem MS, due to ion suppression or the high complexity of the samples [74]. Therefore, these limitations can be overcome by a combination of MSI with classical proteomic methodologies such as liquid chromatography coupled to mass spectrometry (LC-MS). In this method, one tissue section is usually analyzed by MSI, while an adjacent section is homogenized and analyzed by LC–MS/MS in order to identify those molecules that are firstly detected by imaging. This approach has recently been applied to lipids [75], peptides [76,77] and proteins [78,79]. A new strategy for protein identification is the combination of localized *on-tissue* protein digestion and liquid microextraction followed by LC-MS/MS analysis. Here, a chemical inkjet printer is firstly used to perform *on-tissue* microdigestion on selected ROI of the tissue. Then, the tryptic peptides of the region are extracted using an appropriate solvent by liquid microjunction. Finally, the resulting tryptic peptides are subjected to LC separation prior to MS/MS identification. This innovative technique has been successfully used on frozen and FFPE tissue sections [80,81]. Accurate mass measurements also enable the identification of thousands of molecules in a single analysis. In this strategy, MS analysis is performed on a high resolution mass spectrometer to obtain accurate mass measurements of the analytes of interest. Then, the information from the analysis is compared to a reference database (see above for the databases). Finally, histological and molecular biology techniques such as immunohistochemistry, western blot or even quantitative RT-

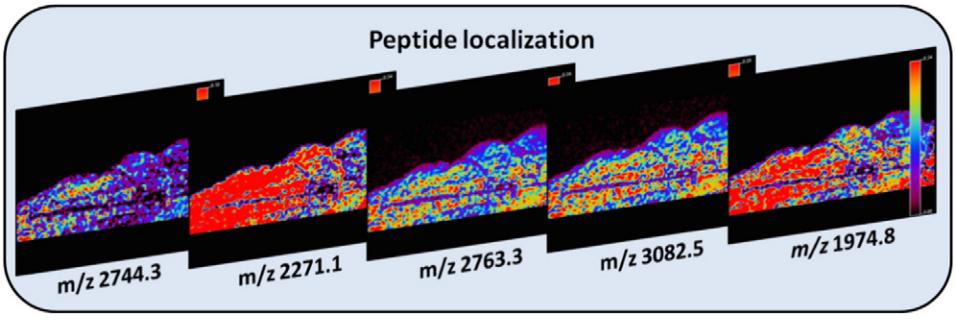

Fig. 2. MALDI-MSI of peptides identified in osteoarthritic cartilage samples using Biomap. Ion distribution of five tryptic peptides corresponding to five different proteins: prolargin (*m/z* 2744.3), aggrecan (*m/z* 2271.1), decorin (*m/z* 2763.3), biglycan (*m/z* 3082.5) and bromodomain and PHD finger-containing protein 3 (*m/z* 1974.8).

PCR offer alternative methods to confirm and validate the abundance or distribution of the target molecules in the tissue [82].

3. MALDI-MSI-based studies in rheumatic diseases

MSI has recently begun to be applied for investigating joint tissues and rheumatology disorders. Fig. 3 illustrates a representative result obtained by MALDI-MSI analysis on human articular cartilage. For instance, MALDI-MSI has been successfully employed for the first time on cartilage to explore the differences in the lipid composition and distribution between healthy and osteoarthritic (OA) tissue [83]. Other MSI studies using the TOF-SIMS strategy have focused on synovial membrane and bone, and also on the molecular characterization of mesenchymal stem cells (MSCs) undergoing chondrogenic differentiation. A summary of the approaches performed to date in this field is presented in Table 2.

3.1. MALDI-MSI analysis of cartilage

Articular cartilage is a connective tissue comprising a unique type of cells, chondrocytes, which are surrounded by an extensive extracellular matrix (ECM). Progressive articular cartilage degradation is the main process that characterizes osteoarthritis (OA) pathophysiology. This process is driven by different molecular mechanisms such as the activation of matrix metalloproteinases (MMPs), aggrecanases and other enzymes, which are responsible for the degradation of ECM [84]. However, OA is a systemic disease that affects the whole joint, including cartilage, synovium, tendons, muscles and subchondral bone [85,86].

Using MSI, recent studies have been conducted to provide information about the identification and localization of proteins, tryptic peptides and lipids from articular cartilage, either healthy or osteoarthritic. Representative proteins that have been identified in MALDI-MSI analysis of cartilage samples are summarized in Table 3. Among these, fibronectin (FN) has been extensively identified in OA cartilage [18,19]. FN is an ECM glycoprotein that has been associated with enhanced levels of catabolic cytokines and up regulation of MMPs involved in OA disease [87]. FN is present at low levels in the ECM of control cartilage but its expression is higher in OA cartilage which produces a change in chondrocyte phenotype and in the activity of MMPs. In fact, several tryptic peptides of FN have shown a higher presence in human OA cartilage compared to healthy tissues [18]. In another work, some of the FN peptides described above displayed a stronger intensity in equine OA cartilage versus young and old cartilage [19]. The higher intensity of FN peptides in OA cartilage was verified using immunohistochemistry. In addition, FN has shown a different distribution pattern within cartilage, being more abundant in the deep area than in the tissue surface [18]. Previous immunoassay studies have reported that FN is highly abundant in the deep area of bovine articular explants [88]. More recently, this protein has been detected in equine articular cartilage by classical immunostaining showing a higher expression in the deep zone compared to either superficial or middle layers [89]. Furthermore, tryptic peptides of COMP have been also identified in OA cartilage by MALDI-MSI, also preferably localized in the deep area of the tissue. COMP has been suggested as a potential biomarker for OA and it has been detected in cartilage secretome [90,91] synovial fluid [92,93], serum [94,95] and urine [96] from human and equine OA patients using classical proteomics. In addition, high levels of COMP in OA cartilage compared to control tissue have been recently displayed by an iTRAQ-based quantitative proteomic analysis [97].Another ECM-related protein identified in OA cartilage is fibromodulin (FM). Many tryptic peptides of FM were found increased in OA samples compared to healthy tissues [18]. Some of these peptides, such as *m/z* 2256.1 of COMP and *m/z* 1361.7 of FM were identified as being distinctive for old equine samples compared to young and OA cartilage, whereas a peptide of collectin-43 protein was specific of young cartilage [19]. Other ECM proteins such as aggrecan core protein, biglycan, prolargin, collagen α 1(II) chain and matrilin-3 were also detected and localized in cartilage by MSI (Table 3).

Glycans are polysaccharides that are mainly found attached to glycoproteins located on the cell surface, in the ECM or serum. The most common glycans in cartilage are *N*-glycans that are attached to ECM proteins such as CD44 or integrins. Structure modifications of *N*-glycans have been related to the pathogenesis of various rheumatic diseases such as RA or OA. For instance, it has been described that changes in the *N*-glycan structure of serum IgG molecules contribute to RA progression [106]. In addition, alterations in cartilage *N*-glycans have been reported in the early phases in a rabbit model of OA [107]. MALDI-MSI has been recently employed to spatially characterize the N-glycome in the cartilage and subchondral bone of knee OA patients [100]. In this study, more than 50 *N*-glycan structures were identified from cartilage and subchondral bone proteins. Among them, high mannose N-glycans showed differential spatial distribution through the OA tissues. Particularly, $(Man)_3 + (Man)_3\ (GlcNAc)_2$ was found increased in cartilage compared to subchondral bone. Other examples were $(NeuAc)_1(Hex)_2\ (HexNAc)_2 + (Man)_3\ (GlcNAc)_2$, only detected in cartilage and $(NeuAc)_2(Hex)_2\ (HexNAc)_2 + (Man)_3\ (GlcNAc)_2$ detected in the bone marrow of the subchondral bone. Alterations in high manosse type *N*-glycans have been also detected in human OA cartilage and degraded mouse cartilage by High-Performance LC-MS [108]. Here, a significantly decrease of high-mannose *N*-glycans in human OA cartilage compared with control cartilage were reported.

3.2. MALDI-MSI analysis of synovial membrane

Inflammation of the synovium results in synovitis, a process commonly associated with rheumatology diseases such as arthritis rheumatoid (RA) and osteoarthritis (OA). Synovitis can occur in early stages of OA [85] but the prevalence and severity of synovium inflammation increases in advanced OA [109]. In addition, OA synovium shows histological changes when compared to normal individuals, such as hyperplasia,

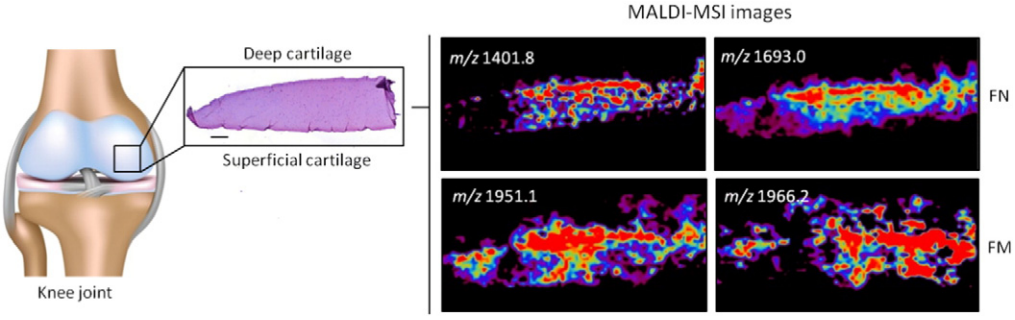

Fig. 3. Representative MALDI-MSI analysis of tissue sections from the human articular cartilage. In the pictures, two tryptic peptides of fibronectin (FN, *m/z* 1401.8 and 1693.0) and fibromodulin (FM, *m/z* 1951.1 and 1966.2) are specifically detected and visualized by MSI in these samples. Significant differences on its abundance can be observed between deep and superficial zones of cartilage tissue.

Table 2
MSI-based studies performed to date on cartilage, synovial membrane and bone.

Tissue	Origin	Disease explored	Target molecules	MSI technique	Validation	Ref.
Cartilage	Human	OA	Peptides/Proteins	MALDI-MSI	IHC	[18]
	Human	Not mentioned (Meniscal lesions)	Peptide/Proteins	MALDI-MSI	Berlin blue staining	[98]
	Human	OA	Lipids	TOF-SIMS	Oil Red staining	[83]
	Equine	OA	Peptides/Proteins	MALDI-MSI	IHC	[19]
	Human (MSCs)	OA (chondrogenic differentiation)	Lipids	MALDI-MSI and TOF-SIMS	Real-Time PCR	[60]
	Human (MSCs and chondrocytes)	OA (chondrogenic differentiation)	Lipids	TOF-SIMS	Oil Red staining/ Real-Time PCR	[99]
	Human	OA	*N*-glycans	MALDI-MSI	–	[100]
Synovial membrane	Human	OA	Peptides/Proteins	MALDI-MSI	IHC	[20]
	Human	OA/RA	Peptides/Proteins	MALDI-MSI	–	[38]
	Human	Haemophilic arthropathy	Peptides/Proteins	MALDI-MSI	Berlin blue staining	[21]
Bone	Rat	Osteoporosis	Calcium/HAp	TOF-SIMS	–	[101]
	Human (MSCs)	Osteoporosis (osteogenic differentiation)	Strontium	TOF-SIMS	–	[102]
	Human (MSCs)	Not mentioned	Lipids	TOF-SIMS	–	[103]
	Human	Not mentioned	HAp	TOF-SIMS	–	[104]
	Human	Not mentioned	Inorganic/Organic bone components	TOF-SIMS	–	[105]
	Human	OA	*N*-glycans	MALDI-MSI	–	[100]

Abbreviations: HAp, hidroxyapatite; IHC, immunohistochemistry; MALDI-MSI, matrix-assisted laser desorption ionization-mass spectrometry imaging; MSCs, mesenchymal stem cells; OA, osteoarthritis; RA, rheumatoid arthritis; TOF-SIMS, time of flight-secondary ion mass spectrometry.

with an increase in number of synovial lining cells and infiltration of inflammatory cells consisting mainly of macrophages and lymphocytes [85,110]. MALDI MSI analysis has been applied to date for the study of protein distribution in RA, OA and haemophilic arthropathy (HA) synovial membranes. A list of the identified proteins in synovial membrane by MALDI-MSI analysis is shown in Table 3. Interestingly, fibronectin-related tryptic peptides were preferentially identified in OA synovial membranes, showing a specific localization in the hypertrophic sample area, which is characterized by a higher grade of inflammation [20].

Table 3
Representative peptides or proteins identified and localized directly in joint tissues by MALDI-MSI.

Peptide/Protein	Sample	ID in[a]	Ref.
Actin, aortic smooth muscle	Synovium	Ctrl	[20]
Aggrecan core protein	Cartilage	OA	[18]
Aggrecan interglobular domain	Cartilage	OA	[19]
Annexin A2	Synovium	Nb-HA	[21]
Biglycan	Cartilage, Synovium	OA/Ctrl	[18,19,20]
Cartilage intermediate layer protein 1	Cartilage	OA/Old	[18,19]
Cartilage oligomeric matrix protein	Cartilage	OA	[18,19]
Cathepsins B and D	Synovium	Nb-HA	[21]
Collagen alpha 1 (II) chain	Cartilage	OA	[18,19]
Collectin 43	Cartilage	Young	[19]
Condroadherin	Cartilage	OA	[19]
Decorin	Cartilage	Ctrl	[18]
Defensins alpha-1 and -3	Synovium	RA	[38]
Ferritin chains	Synovium/Meniscus	B-HA/HG-L	[21,98]
Fibrinogen chains	Synovium	B-HA	[21]
Fibromodulin	Cartilage	OA	[18,19]
Fibronectin	Cartilage, Synovium	OA	[18,19,20]
Hemoglobin subunits	Cartilage, Synovium	OA/B-HA	[20,21]
Histones H2A2, H2B and H4	Synovium	RA	[38]
Matrilin-3	Cartilage	OA	[19]
Melanoma inhibitory activity 3	Cartilage	OA	[19]
Prolargin	Cartilage	OA/Ctrl	[18]
Protein ELYS	Cartilage	OA	[18]
S100 A11 (calgizzarin)	Synovium	RA	[38]
S100 A6 (calcyclin)	Synovium	RA	[38]
S100 A8 (calgranulin A)	Synovium	RA	[38]
Thymosins beta-4 and −10	Synovium	RA	[38]

[a] Condition in which the protein was preferentially identified. Abbreviations: B-HA, bleeding areas in haemophilic arthropathy; Ctrl, healthy controls; Nb-HA, non-bleeding areas in haemophilic arthropathy; HG-L, lesions with high grade of degeneration.

These peptides were previously described by MSI in OA-affected cartilage [18]. Therefore, these findings suggest that FN is common to OA samples (cartilage and synovium) and could be used as biomarker to discriminate between healthy and OA-related tissues using this methodology. On the other hand, thymosin beta-related native peptides were mainly found in RA synovial membranes, displaying a strong intensity in the synovial sublining layer [38]. In the same study, a higher intensity of defensin alpha-related native peptides was found in RA tissue samples. These peptides were localized in both synovial membrane layers after MALDI-MSI measurements. Finally, many other proteins were described by MSI in RA synovial membranes, including members of the S100 protein family such as S100 A6 or S100 A11 and several histones [20].

Haemophilic arthropathy is a rheumatic disease caused by repeated bleeding into the joint of patients with haemophilia [111]. It is characterized by synovial inflammation and cartilage and bone destruction, features of degenerative joint diseases, such as OA an RA [112–115]. In addition, bleeding may lead to osteoclast activation and bone resorption [116]. The resulting decrease in bone mineral density induces osteoporosis, another rheumatology disease which has been associated with haemophilic arthropathy [117]. To explore the pathogenesis mechanisms of this disease, the protein profile of synovial membranes from patients affected by HA has been characterized by MSI [21]. This has allowed to discriminate between bleeding and non-bleeding areas within the synovium, by associating differential protein patterns to the specific zones: for instance, ferritin chains, several hemoglobin subunits, fibrinogen and truncated coagulation factor VIII tryptic peptides were mainly localized in the bleeding tissue areas, whereas tryptic peptides of annexin A2, and cathepsins were more abundant in areas without blood.

3.3. MALDI-MSI analysis of meniscus

Recently, meniscal lesions have been also characterized by MALDI-MSI [98]. It has been shown that traumatic and degenerative meniscal lesions led to knee osteoarthritis [118]. In this work, MALDI-MSI analysis has allowed to discriminate acute (areas with high-grade of degeneration) and non-acute (areas with low-grade of degeneration) meniscal lesions, by associating differential peptide profiles to these specific areas. Tryptic peptides such as *m/z* 1151.6, 1431.7 and 1927.1 were mainly detected in the high-grade degenerated areas whereas *m/z* 1356.0, 1138.0 and 1303.0 were only identified in the meniscal areas

with low-grade of degeneration. In addition, ferritin light (*m/z* 676 and 1608) and heavy chains (*m/z* 658 and 1345) were found in the acute meniscal tissue. The detection of ferritin in the meniscus is a clear indication of a previous strong trauma.

3.4. MALDI-MSI analysis of mesenchymal stem cells undergoing chondrogenesis

A different research topic intimately related with cartilage is chondrogenesis, the process by which mesenchymal stem cells (MSCs) differentiate towards chondrocytes and begin to secrete the molecules that form the extracellular matrix of cartilage [119]. Alterations in chondrogenesis have been associated with OA pathology, thus this process has been recently proposed as a new target for disease-modifying OA drugs (DMOADs) or chondroprotective treatments [120]. Following this reasoning, DMOAD agents would be able to induce chondrogenesis, encouraging the reparation of damaged articular cartilage. Therefore, gaining knowledge on this differentiation process would be very valuable not only for a better understanding of cartilage biology, but also to facilitate the development of novel therapeutic strategies for OA.

Focused in chondrogenesis, MSI analyses have been performed to date with the aim of characterizing the spatial distribution of lipids in human bone marrow MSCs (hBMSCs) during their differentiation towards chondrocyte-like cells after 2 and 14 days of chondrogenic induction [60]. In this work, phosphocholine-related species have been identified in hBMSCs monocultures after 2 days of chondrogenesis using MALDI-MSI. Other lipids specifically increased during the undifferentiated chondrogenic stage (day 2) were sphingomyelins (SMs), whereas unsaturated fatty acids (FA) such as arachidonic acid and docosohexaenoic acid were only detected after 14 days of differentiation. In addition, several types of phospholipids such as phosphatidylethanolamines (PE) and phosphatidylinositols (PI) were also predominantly identified at day 14 of chondrogenesis. A summary of the lipids identified by MALDI-MSI in MSCs is shown in Table 4.

Table 4
Representative lipids identified and localized directly in MSCs undergoing chondrogenesis by MALDI-MSI.

Lipid name	Observed *m/z* ratio	Condition
Choline	104.1	Day 2
Sodiated headgroup of PC	146.9	Day 2
Dehydrated phosphoglycerol	153.0	Day 14
Potassiated headgroup of PC	162.9	Day 2
Phosphocholine	184.1	Day 2
Phosphocholine-related ion	198.1	Day 2
Inositol monophosphate	259.0	Day 14
Arachidonic acid (C20:4)	303.2	Day 14
Docosahexaenoic acid (C22:6)	327.2	Day 14
Lipid fragments		
PC (C16:0/C18:1)	478.3	Day 2
PC (C16:0/C18:1)	504.3	Day 2
SM (d18:1/C16:0)	542.5	Day 2
PC (C16:0/C18:1)	577.5	Day 2
PC (C16:0/C18:1)	599.5	Day 2
SM (C18:1/C16:0)	666.5	Day 2
Sphingolipids		
SM (d18:1/C16:0-N$(CH_3)_3$	682.5	Day 2
SM (d18:1/C16:1)	723.5	Day 2
SM (d18:1/C16:0)	725.5	Day 2
SM (d18:1/C18:1)	729.5	Day 14
SM (d18:1/C16:0)	741.5	Day 2
SM (d18:1/C19:0)/SM (d18:1/C18:1)	767.5	Day 2
SM (d18:1/C24:0)	853.6	Day 2
ST (d18:1/C16:0)	778.5	Day 14
Glycerolipids (GLs)		
PC (C16:0/C18:1-N$(CH_3)_3$	739.5	Day 2
PC (C16:0/C18:1)	782.6	Day 2
PC (C18:0/C18:0)	790.5	Day 14
PC (C16:0/C18:1)	798.5	Day 2
PC (C34:0)	800.5	Day 2
PC (C36:2)	824.5	Day 2
PC (C18:0/C18:1)	826.6	Day 2
PC (C18:4/C20:0)	832.5	Day 14
PE (C18:0/C20:4)	750.5	Day 14
PE (C18:0/C22:4)	794.5	Day 14
PI (C18:1/C20:4)	883.6	Day 2
PI (C18:0/C20:4)	885.6	Day 14
PI (C42:3)	943.5	Day 14
PG (C18:1/C22:6)	819.5	Day 14

PC: phosphatidylcholine; SM: sphingomyelins; PE: phosphatidylethanolamine; ST: sulfatide; PG: phosphatidylglycerol; PI: phosphatidylinositol. Reproduced from Ref. 46.

4. Analysis of joint-derived tissues using other MSI techniques

Apart from MALDI, other ionization techniques have been used to explore tissues or cells related with rheumatic disorders by MSI analysis. These include analysis of lipids in cartilage by TOF-SIMS, and also studies on mesenchymal stem cells subjected to chondrogenic inducers and on osteoporotic bone.

4.1. MSI analysis of cartilage by TOF-SIMS

OA is a chronic systemic musculoskeletal disorder involving inflammation, immunity as well as metabolic alterations [121]. Recent investigations suggest that a wide variety of lipid mediators, including fatty acids, sphingolipids, and glycerolipids, are potentially involved in the pathophysiology of cartilage degradation in OA and in other arthritic diseases such as RA [122,123]. TOF-SIMS is becoming a more and more common analytical platform for lipid and metabolite imaging. Even if this technique is limited to small molecules (typically below 1000 Da), it offers enough sensitivity to detect and locate several lipids directly on the surface of tissue sections and cells [124,125]. Accordingly, TOF-SIMS technology has been recently applied to investigate the composition and distribution of lipids in osteoarthritic cartilage [83]. The lipid species identified directly from cartilage sections include vitamin D-3 and several glycerolipids such as monoacylglycerols (MAGs) and diacylglycerols (DAGs) [83]. Interestingly, all these lipids were directly identified in OA cartilage and localized in the superficial region of the tissue. In addition, several cholesterol species have been observed in the superficial ECM of the OA cartilage compared to the deep area, as well as several saturated and unsaturated FA such as oleic acid (*m/z* 281.2), pamitic acid (*m/z* 255.2) or stearic acid (*m/z* 283.1). Generally, all these FA were located in the cholesterol-rich area. This increased amount of lipids in the diseased tissue was also detected through the observation of lipid droplets in the superficial area of the OA cartilage by Oil red staining [83]. Several proteomic-based studies have supported a high lipid deposition during OA. For instance, several FA, DAGs and other lipids have been detected in high concentrations in the plasma of OA patients by liquid chromatography (LC) [126]. In addition, different metabolites involved in the metabolism of FA and lipids, identified by ultra-performance LC-MS, have been found significantly altered in the serum of OA patients compared to control donors [128]. Free FA have been described as potential proinflamatory mediators in joint diseases [127]. In fact, it has been recently reported that stearic acid induces proinflamatory cytokine production partly through the activation of a novel lactate-HIF1α pathway in chondrocytes [129]. Moreover, chondrocyte apoptosis and articular cartilage degradation can also be induced by palmitic acid in synergy with interleukin 1 β citokine [130].

4.2. TOF-SIMS MSI analysis of mesenchymal stem cells undergoing chondrogenesis

An evaluation of the changes in the lipid profiles during chondrogenesis has also been conducted by Georgi and co-workers [99], who analyzed cocultures and monocultures of hBMSCs and primary chondrocytes under normoxic and hypoxic conditions using TOF-SIMS. Normoxic cultures revealed a higher lipid content compared to

those cells cultured under hypoxic conditions, a finding that was verified by Oil Red staining. In addition, several cholesterol species displayed a higher intensity in normoxic culture pellets. Moreover, many DAGs were predominantly expressed in cultures containing MSCs, whereas phosphocholine was increased in chondrocytes monocultures. Finally, a higher glycosaminoglycan deposition in co-cultures of hBMSCs and chondrocytes under normoxia was observed, indicating a better cartilage formation in normoxic conditions compared to cocultures in hypoxia. This decrease in chondrogenesis in hypoxic conditions was associated with a decrease in the mRNA expression of the chondrogenic marker SOX9, as well as in the expression of fibroblast growth factor 1 (FGF-1). Moreover, the loss in cartilage formation was also attributed to the lower content of lipids, especially cholesterol. The application of TOF-SIMS has revealed variations in the lipid localization between different stages of chondrogenesis [60]. For instance, phosphocholine-related ions were predominantly expressed in the peripheral cells, suggesting a more advanced differentiation of the cells situated in the micromass core. In addition, TOF-SIMS experiments showed that several MAGs, DAGs, and ceramide lipid classes are more abundant in advanced stages of chondrogenesis.

4.3. MSI analysis of bone

Bone is a highly vascular, connective tissue formed by different cells such as osteoblasts (bone formation), osteocytes (bone remodeling and mineralization) and osteoclasts (bone reabsorption), and the mineralized ECM. Bone ECM has an organic component, mainly composed of type I collagen, lipids, non-collagenous proteins and proteoglycans, and an inorganic fraction formed by different salts such as phosphates and calcium carbonates. Changes in the composition of the tissue have been associated to rheumatic diseases such as osteoporosis [131] and OA [132], as well to other disorders such as Turner's syndrome [133] [134] or osteogenesis imperfecta [135]. For instance, calcium (Ca) distribution and concentration in bone is essential for the assessment of bone quality, enabling the diagnosis of osteoporosis. This latter disease is characterized by a decreased bone mineral density (BMD) and a loss of bone quality, which significantly increase the risk of bone fracture [136].

Recent MSI-based studies have been carried out to optimize preparation protocols for the molecular characterization of bone [103] [105], whereas other works have been performed to investigate structural variations and changes on the mineral content and distribution in bone cells and tissue. The biomolecules identified in these studies include several hydroxyapatite fragments, which have been preferentially observed in mineralized bone areas after TOF-SIMS analysis [101,104,137]. Furthermore, a decrease of several calcium phosphate ions generated from hydroxyapatite has been observed in bone affected by osteoporosis, compared to healthy tissue. The distribution of these different calcium phosphate molecules within the bone has been evaluated through the Ca/P ratio, showing that the mineralization areas of the osteoporotic bone display a lower Ca/P ratio compared to healthy [101]. A decrease in calcium content and an alteration on its distribution have been also described by TOF-SIMS in osteoporotic bone [101], since Ca concentration found to be lower in the edge region than in the centre of the trabecula.

Apart from calcium, strontium (Sr) content has been also characterized by TOF-SIMS, in this case in bone cells during osteogenic differentiation [102]. A high Sr content inside osteogenically differentiated hMSCs that were expanded in different Sr-enriched bone cements was observed. Moreover, a very high Sr signal was also found in the mineralized ECM of those osteoblast-like cells cultured in the bone cements mentioned above. Strontium (Sr) could have potential application in the treatment of osteoporosis because of their antiresorptive effect [138]. In fact, there is currently a high interest in the development of Sr-enriched biomaterials as promising implant materials for the osteoporotic bone.

5. Conclusions

Taken all together, MALDI-MSI methods carried out to date have identified and localized many proteins that may relate to pathological mechanisms of rheumatic diseases such as OA, RA or haemophilic arthropathy. TOF-SIMS analyses have also highlighted the relevant role of lipid metabolism in joint-related diseases. The results obtained demonstrate the usefulness of this technology as a novel source of information about pathogenesis of rheumatic diseases. Although still technological improvements need to be made, MALDI-MSI is a promising tool for rheumatology research in order to gain better knowledge on disease pathogenesis and describe novel biological markers of the disease state.

Transparency Document

The Transparency document associated with this article can be found, in the online version.

Acknowledgements

This work was funded by grants from Fondo Investigación Sanitaria-Spain (PI12/00329, PI14/01707, CIBER-CB06/01/0040, RETIC-RIER-RD12/0009/0018). C.R.-R. is supported by the Miguel Servet II program from Fondo Investigación Sanitaria-Spain (CPII15/00013). The Proteomics Unit belongs to ProteoRed, PRB2- ISCIII, supported by grant PT13/0001.

References

[1] C. Eriksson, N. Masaki, I. Yao, T. Hayasaka, M. Setou, MALDI imaging mass spectrometry-a mini review of methods and recent developments, Mass Spectrom. 2 (2013) S0022 Spec Iss.
[2] P. Chaurand, Imaging mass spectrometry of thin tissue sections: a decade of collective efforts, J. Proteome 75 (16) (2012) 4883–4892.
[3] D. Gode, D.A. Volmer, Lipid imaging by mass spectrometry - a review, Analyst 138 (5) (2013) 1289–1315.
[4] C.N. Ferguson, J.W. Fowler, J.F. Waxer, R.A. Gatti, J.A. Loo, Mass spectrometry-based tissue imaging of small molecules, Adv. Exp. Med. Biol. 806 (2014) 283–299.
[5] H. Gagnon, J. Franck, M. Wisztorski, R. Day, I. Fournier, M. Salzet, Prog. Histochem. Cytochem. 47 (3) (2012) 133–174.
[6] M.R. Groseclose, P.P. Massion, P. Chaurand, R.M. Caprioli, High-throughput proteomic analysis of formalin-fixed paraffin-embedded tissue microarrays using MALDI imaging mass spectrometry, Proteomics 8 (18) (2008) 3715–3724.
[7] R. Casadonte, R.M. Caprioli, Proteomic analysis of formalin-fixed paraffin-embedded tissue by MALDI imaging mass spectrometry, Nat. Protoc. 6 (11) (2011) 1695–1709.
[8] M. Svensson, M. Boren, K. Sköld, M. Fälth, B. Sjögren, M. Andersson, et al., Heat stabilization of the tissue proteome: a new technology for improved proteomics, J. Proteome Res. 8 (2) (2009) 974–981.
[9] R.J. Goodwin, A.M. Lang, H. Allingham, M. Borén, A.R. Pitt, Stopping the clock on proteomic degradation by heat treatment at the point of tissue excision, Proteomics 10 (9) (2010) 1751–1761.
[10] R.M. Caprioli, T.B. Farmer, J. Gile, Molecular imaging of biological samples: localization of peptides and proteins using MALDI-TOF MS, Anal. Chem. 69 (23) (1997) 4751–4760.
[11] S.A. Schwartz, M.L. Reyzer, R.M. Caprioli, Direct tissue analysis using matrix-assisted laser desorption/ionization mass spectrometry: practical aspects of sample preparation, J. Mass Spectrom. 38 (7) (2003) 699–708.
[12] A.C. Crecelius, D.S. Cornett, R.M. Caprioli, B. Williams, B.M. Dawant, B. Bodenheimer, Three-dimensional visualization of protein expression in mouse brain structures using imaging mass spectrometry, J. Am. Soc. Mass Spectrom. 16 (7) (2005) 1093–1099.
[13] P. Chaurand, S.A. Schwartz, D. Billheimer, B.J. Xu, A. Crecelius, R.M. Caprioli, Integrating histology and imaging mass spectrometry, Anal. Chem. 76 (4) (2004) 1145–1155.
[14] K. Chughtai, L. Jiang, T.R. Greenwood, K. Glunde, R.M. Heeren, Mass spectrometry images acylcarnitines, phosphatidylcholines, and sphingomyelin in MDA-MB-231 breast tumor models, J. Lipid Res. 54 (2) (2013) 333–344.
[15] F. Deutskens, J. Yang, R.M. Caprioli, High spatial resolution imaging mass spectrometry and classical histology on a single tissue section, J. Mass Spectrom. 46 (6) (2011) 568–571.

[16] E.H. Seeley, S.R. Oppenheimer, D. Mi, P. Chaurand, R.M. Caprioli, Enhancement of protein sensitivity for MALDI imaging mass spectrometry after chemical treatment of tissue sections, J. Am. Soc. Mass Spectrom. 19 (8) (2008) 1069–1077.

[17] A. Thomas, N.H. Patterson, J. Laveaux Charbonneau, P. Chaurand, Orthogonal organic and aqueous-based washes of tissue sections to enhance protein sensitivity by MALDI imaging mass spectrometry, J. Mass Spectrom. 48 (1) (2013) 42–48.

[18] B. Cillero-Pastor, G.B. Eijkel, A. Kiss, F.J. Blanco, R.M. Heeren, Matrix-assisted laser desorption ionization-imaging mass spectrometry: a new methodology to study human osteoarthritic cartilage, Arthritis Rheum. 65 (3) (2013) 710–720.

[19] M.J. Peffers, B. Cillero-Pastor, G.B. Eijkel, P.D. Clegg, R.M. Heeren, Matrix assisted laser desorption ionization mass spectrometry imaging identifies markers of ageing and osteoarthritic cartilage, Arthritis Res. Ther. 16 (3) (2014) R110.

[20] B. Cillero-Pastor, G.B. Eijkel, F.J. Blanco, R.M. Heeren, Protein classification and distribution in osteoarthritic human synovial tissue by matrix-assisted laser desorption ionization mass spectrometry imaging, Anal. Bioanal. Chem. 407 (8) (2015) 2213–2222.

[21] M. Kriegsmann, R. Casadonte, T. Randau, S. Gravius, P. Pennekamp, A. Strauss, et al., MALDI imaging of predictive ferritin, fibrinogen and proteases in haemophilic arthropathy, Haemophilia 20 (3) (2014) 446–453.

[22] Y. Aoki, A. Toyama, T. Shimada, T. Sugita, C. Aoki, Y. Umino, et al., A novel method for analyzing formalin-fixed paraffin embedded (FFPE) tissue sections by mass spectrometry imaging, Proc. Jpn. Acad. Ser. B Phys. Biol. Sci. 83 (7) (2007) 205–214.

[23] S. Yamashita, Heat-induced antigen retrieval: mechanisms and application to histochemistry, Prog. Histochem. Cytochem. 41 (3) (2007) 141–200.

[24] J.O. Gustafsson, M.K. Oehler, S.R. McColl, P. Hoffmann, Citric acid antigen retrieval (CAAR) for tryptic peptide imaging directly on archived formalin-fixed paraffin-embedded tissue, J. Proteome Res. 9 (9) (2010) 4315–4328.

[25] E.R. van Hove, D.F. Smith, L. Fornai, K. Glunde, R.M. Heeren, An alternative paper based tissue washing method for mass spectrometry imaging: localized washing and fragile tissue analysis, J. Am. Soc. Mass Spectrom. 22 (10) (2011) 1885–1890.

[26] G. De Sio, A.J. Smith, M. Galli, M. Garancini, C. Chinello, F. Bono, et al., A MALDI-mass spectrometry imaging method applicable to different formalin-fixed paraffin-embedded human tissues, Mol. BioSyst. 11 (6) (2015) 1507–1514.

[27] M. Pietrowska, M. Gawin, J. Polańska, P. Widłak, Tissue fixed with formalin and processed without paraffin embedding is suitable for imaging of both peptides and lipids by MALDI-IMS, Proteomics 16 (11–12) (2016) 1670–1677.

[28] H.C. Diehl, B. Beine, J. Elm, D. Trede, M. Ahrens, M. Eisenacher, et al., The challenge of on-tissue digestion for MALDI MSI- a comparison of different protocols to improve imaging experiments, Anal. Bioanal. Chem. 407 (8) (2015) 2223–2243.

[29] O.J. Gustafsson, J.S. Eddes, S. Meding, S.R. McColl, M.K. Oehler, P. Hoffmann, Matrix-assisted laser desorption/ionization imaging protocol for in situ characterization of tryptic peptide identity and distribution in formalin-fixed tissue, Rapid Commun. Mass Spectrom. 27 (6) (2013) 655–670.

[30] M.C. Djidja, S. Francese, P.M. Loadman, C.W. Sutton, P. Scriven, E. Claude, et al., Detergent addition to tryptic digests and ion mobility separation prior to MS/MS improves peptide yield and protein identification for in situ proteomic investigation of frozen and formalin-fixed paraffin-embedded adenocarcinoma tissue sections, Proteomics 9 (10) (2009) 2750–2763.

[31] B. Enthaler, M. Trusch, M. Fischer, C. Rapp, J.K. Pruns, J.P. Vietzke, MALDI imaging in human skin tissue sections: focus on various matrices and enzymes, Anal. Bioanal. Chem. 405 (4) (2013) 1159–1170.

[32] K.R. Tucker, L.A. Serebryannyy, T.A. Zimmerman, S.S. Rubakhin, J.V. Sweedler, The modified-bead stretched sample method: development and application to MALDI-MS imaging of protein localization in the spinal cord, Chem. Sci. 2 (4) (2011) 785–795.

[33] M.R. Groseclose, M. Andersson, W.M. Hardesty, R.M. Caprioli, Identification of proteins directly from tissue: in situ tryptic digestions coupled with imaging mass spectrometry, J. Mass Spectrom. 42 (2) (2007) 254–262.

[34] B.K. Kaletaş, I.M. van der Wiel, J. Stauber, C. Güzel, J.M. Kros, T.M. Luider, et al., Sample preparation issues for tissue imaging by imaging MS, Proteomics 9 (10) (2009) 2622–2633.

[35] Y. Schober, S. Guenther, B. Spengler, A. Römpp, High-resolution matrix-assisted laser desorption/ionization imaging of tryptic peptides from tissue, Rapid Commun. Mass Spectrom. 26 (9) (2012) 1141–1146.

[36] V. Mainini, G. Bovo, C. Chinello, E. Gianazza, M. Grasso, G. Cattoretti, et al., Detection of high molecular weight proteins by MALDI imaging mass spectrometry, Mol. BioSyst. 9 (6) (2013) 1101–1107.

[37] A. van Remoortere, R.J. van Zeijl, N. van den Oever, J. Franck, R. Longuespée, M. Wisztorski, et al., MALDI imaging and profiling MS of higher mass proteins from tissue, J. Am. Soc. Mass Spectrom. 21 (11) (2010) 1922–1929.

[38] M. Kriegsmann, E.H. Seeley, A. Schwarting, J. Kriegsmann, M. Otto, H. Thabe, et al., MALDI MS imaging as a powerful tool for investigating synovial tissue, Scand. J. Rheumatol. 41 (4) (2012) 305–309.

[39] X. Wang, J. Han, D.B. Hardie, J. Yang, C.H. Borchers, The use of matrix coating assisted by an electric field (MCAEF) to enhance mass spectrometric imaging of human prostate cancer biomarkers, J. Mass Spectrom. 51 (1) (2016) 86–95.

[40] R. Lemaire, A. Desmons, J.C. Tabet, R. Day, M. Salzet, I. Fournier, Direct analysis and MALDI imaging of formalin-fixed, paraffin-embedded tissue sections, J. Proteome Res. 6 (4) (2007) 1295–1305.

[41] C. Pan, S. Xu, H. Zhou, Y. Fu, M. Ye, H. Zou, Recent developments in methods and technology for analysis of biological samples by MALDI-TOF-MS, Anal. Bioanal. Chem. 387 (1) (2007) 193–204.

[42] A. Tholey, E. Heinzle, Ionic (liquid) matrices for matrix-assisted laser desorption/ionization mass spectrometry-applications and perspectives, Anal. Bioanal. Chem. 386 (1) (2006) 24–37.

[43] K.D. Herring, S.R. Oppenheimer, R.M. Caprioli, Direct tissue analysis by matrix-assisted laser desorption ionization mass spectrometry: application to kidney biology, Semin. Nephrol. 27 (6) (2007) 597–608.

[44] D.A. Stoyanovsky, L.J. Sparvero, A.A. Amoscato, R.R. He, S. Watkins, B.R. Pitt, et al., Improved spatial resolution of matrix-assisted laser desorption/ionization imaging of lipids in the brain by alkylated derivatives of 2,5-dihydroxybenzoic acid, Rapid Commun. Mass Spectrom. 28 (5) (2014) 403–412.

[45] R. Lemaire, J.C. Tabet, P. Ducoroy, J.B. Hendra, M. Salzet, I. Fournier, Solid ionic matrixes for direct tissue analysis and MALDI imaging, Anal. Chem. 78 (3) (2006) 809–819.

[46] K. Shrivas, T. Hayasaka, N. Goto-Inoue, Y. Sugiura, N. Zaima, M. Setou, Ionic matrix for enhanced MALDI imaging mass spectrometry for identification of phospholipids in mouse liver and cerebellum tissue sections, Anal. Chem. 82 (21) (2010) 8800–8806.

[47] G. Stübiger, O. Belgacem, Analysis of lipids using 2,4,6-trihydroxyacetophenone as a matrix for MALDI mass spectrometry, Anal. Chem. 79 (2007) 3206–3213.

[48] C.D. Cerruti, F. Benabdellah, O. Laprévote, D. Touboul, A. Brunelle, MALDI imaging and structural analysis of rat brain lipid negative ions with 9-aminoacridine matrix, Anal. Chem. 84 (5) (2012) 2164–2171.

[49] R.T. Steven, A.M. Race, J. Bunch, Para-nitroaniline is a promising matrix for MALDI-MS imaging on intermediate pressure MS systems, J. Am. Soc. Mass Spectrom. 24 (5) (2013) 801–804.

[50] E.A. Jones, S.O. Deininger, P.C. Hogendoorn, A.M. Deelder, L.A. McDonnell, Imaging mass spectrometry statistical analysis, J. Proteome 75 (16) (2012) 4962–4989.

[51] J.L. Norris, D.S. Cornett, J.A. Mobley, M. Andersson, E.H. Seeley, P. Chaurand, et al., Processing MALDI mass spectra to improve mass spectral direct tissue analysis, Int. J. Mass Spectrom. 260 (2–3) (2007) 212–221.

[52] M. Hanselmann, U. Köthe, M. Kirchner, B.Y. Renard, E.R. Amstalden, K. Glunde, et al., Toward digital staining using imaging mass spectrometry and random forests, J. Proteome Res. 8 (7) (2009) 3558–3567.

[53] S.O. Deininger, D.S. Cornett, R. Paape, M. Becker, C. Pineau, S. Rauser, et al., Normalization in MALDI-TOF imaging datasets of proteins: practical considerations, Anal. Bioanal. Chem. 401 (1) (2011) 167–181.

[54] W. Meuleman, J.Y. Engwegen, M.C. Gast, J.H. Beijnen, M.J. Reinders, L.F. Wessels, Comparison of normalisation methods for surface-enhanced laser desorption and ionisation (SELDI) time-of-flight (TOF) mass spectrometry data, BMC Bioinf. 9 (2008) 88.

[55] T. Alexandrov, MALDI imaging mass spectrometry: statistical data analysis and current computational challenges, BMC Bioinf. 13 (Suppl. 16) (2012) S11.

[56] J.M. Fonville, C. Carter, O. Cloarec, J.K. Nicholson, J.C. Lindon, J. Bunch, et al., Robust data processing and normalization strategy for MALDI mass spectrometric imaging, Anal. Chem. 84 (3) (2012) 1310–1319.

[57] G. Robichaud, K.P. Garrard, J.A. Barry, D.C. Muddiman, MSiReader: an open-source interface to view and analyze high resolving power MS imaging files on Matlab platform, J. Am. Soc. Mass Spectrom. 24 (5) (2013) 718–721.

[58] G. McCombie, D. Staab, M. Stoeckli, R. Knochenmuss, Spatial and spectral correlations in MALDI mass spectrometry images by clustering and multivariate analysis, Anal. Chem. 77 (19) (2005) 6118–6124.

[59] L.A. Klerk, P.Y. Dankers, E.R. Popa, A.W. Bosman, M.E. Sanders, K.A. Reedquist, et al., TOF-secondary ion mass spectrometry imaging of polymeric scaffolds with surrounding tissue after in vivo implantation, Anal. Chem. 82 (11) (2010) 4337–4343.

[60] B. Rocha, B. Cillero-Pastor, G. Eijkel, A.L. Bruinen, C. Ruiz-Romero, R.M. Heeren, et al., Characterization of lipidic markers of chondrogenic differentiation using mass spectrometry imaging, Proteomics 15 (4) (2015) 702–713.

[61] L.A. McDonnell, G.L. Corthals, S.M. Willems, A. van Remoortere, R.J. van Zeijl, A.M. Deelder, Peptide and protein imaging mass spectrometry in cancer research, J. Proteome 73 (10) (2010) 1921–1944.

[62] M.C. Djidja, E. Claude, M.F. Snel, S. Francese, P. Scriven, V. Carolan, et al., Novel molecular tumour classification using MALDI-mass spectrometry imaging of tissue micro-array, Anal. Bioanal. Chem. 397 (2) (2010) 587–601.

[63] B. Cillero-Pastor, R.M. Heeren, Matrix-assisted laser desorption ionization mass spectrometry imaging for peptide and protein analyses: a critical review of on-tissue digestion, J. Proteome Res. 13 (2) (2014) 325–335.

[64] L.A. McDonnell, A. Walch, M. Stoeckli, G.L. Corthals, MSiMass list: a public database of identifications for protein MALDI MS imaging, J. Proteome Res. 13 (2) (2014) 1138–1142.

[65] S.K. Maier, H. Hahne, A.M. Gholami, B. Balluff, S. Meding, C. Schoene, et al., Comprehensive identification of proteins from MALDI imaging, Mol. Cell. Proteomics 12 (10) (2013) 2901–2910.

[66] E. Yasugi, K. Watanabe, LIPIDBANK for Web, the newly developed lipid database, Tanpakushitsu Kakusan Koso 47 (7) (2002) 837–841.

[67] R. Taguchi, M. Nishijima, T. Shimizu, Basic analytical systems for lipidomics by mass spectrometry in Japan, Methods Enzymol. 432 (2007) 185–211.

[68] E. Fahy, M. Sud, D. Cotter, S. Subramaniam, LIPID MAPS online tools for lipid research, Nucleic Acids Res. 35 (2007) W606–W612 Web Server issue.

[69] M. Sud, E. Fahy, D. Cotter, A. Brown, E.A. Dennis, C.K. Glass, et al., LMSD: LIPID MAPS structure database, Nucleic Acids Res. 35 (2007) D527–D532 Database issue.

[70] D.S. Wishart, T. Jewison, A.C. Guo, M. Wilson, C. Knox, Y. Liu, et al., HMDB 3.0–the Human Metabolome Database in 2013, Nucleic Acids Res. 41 (2013) D801–D807 Database issue.

[71] T. Kind, K.H. Liu, dY. Lee, B. DeFelice, J.K. Meissen, O. Fiehn, LipidBlast in silico tandem mass spectrometry database for lipid identification, Nat. Methods 10 (8) (2013) 755–758.

[72] C.A. Smith, G. O'Maille, E.J. Want, C. Qin, S.A. Trauger, T.R. Brandon, et al., METLIN: a metabolite mass spectral database, Ther. Drug Monit. 27 (6) (2005) 747–751.

[73] M. Kanehisa, The KEGG database, Novartis Found Symp, Vol. 247, 2002, pp. 91–101 discussion -3, 19-28, 244-52.

[74] D. Debois, V. Bertrand, L. Quinton, M.C. De Pauw-Gillet, E. De Pauw, MALDI-in source decay applied to mass spectrometry imaging: a new tool for protein identification, Anal. Chem. 82 (10) (2010) 4036–4045.
[75] P. Loziuk, F. Meier, C. Johnson, H.T. Ghashghaei, D.C. Muddiman, TransOmic analysis of forebrain sections in Sp2 conditional knockout embryonic mice using IR-MALDESI imaging of lipids and LC-MS/MS label-free proteomics, Anal. Bioanal. Chem. 408 (13) (2016) 3453–3474.
[76] N.J. Hunt, L. Phillips, K.A. Waters, R. Machaalani, Proteomic MALDI-TOF/TOF-IMS examination of peptide expression in the formalin fixed brainstem and changes in sudden infant death syndrome infants, J. Proteome 138 (2016) 48–60.
[77] B. Chatterji, C. Dickhut, S. Mielke, J. Krüger, I. Just, S. Glage, et al., MALDI imaging mass spectrometry to investigate endogenous peptides in an animal model of Usher's disease, Proteomics 14 (13–14) (2014) 1674–1687.
[78] L. Mourino-Alvarez, I. Iloro, F. de la Cuesta, M. Azkargorta, T. Sastre-Oliva, I. Escobes, et al., MALDI-imaging mass spectrometry: a step forward in the anatomopathological characterization of stenotic aortic valve tissue, Sci. Rep. 6 (2016) 27106.
[79] C.H. Na, J.H. Hong, W.S. Kim, S.R. Shanta, J.Y. Bang, D. Park, et al., Identification of protein markers specific for papillary renal cell carcinoma using imaging mass spectrometry, Mol. Cell 38 (7) (2015) 624–629.
[80] J. Quanico, J. Franck, C. Dauly, K. Strupat, J. Dupuy, R. Day, et al., Development of liquid microjunction extraction strategy for improving protein identification from tissue sections, J. Proteome 79 (2013) 200–218.
[81] M. Wisztorski, B. Fatou, J. Franck, A. Desmons, I. Farré, E. Leblanc, et al., Microproteomics by liquid extraction surface analysis: application to FFPE tissue to study the fimbria region of tubo-ovarian cancer, Proteomics Clin. Appl. 7 (3–4) (2013) 234–240.
[82] V. Rebours, J. Le Faouder, S. Laouirem, M. Mebarki, M. Albuquerque, J.M. Camadro, et al., In situ proteomic analysis by MALDI imaging identifies ubiquitin and thymosin-β4 as markers of malignant intraductal pancreatic mucinous neoplasms, Pancreatology 14 (2) (2014) 117–124.
[83] B. Cillero-Pastor, G. Eijkel, A. Kiss, F.J. Blanco, R.M. Heeren, Time-of-flight secondary ion mass spectrometry-based molecular distribution distinguishing healthy and osteoarthritic human cartilage, Anal. Chem. 84 (21) (2012) 8909–8916.
[84] M.B. Goldring, S.R. Goldring, Osteoarthritis, J. Cell. Physiol. 213 (3) (2007) 626–634.
[85] J. Sellam, F. Berenbaum, The role of synovitis in pathophysiology and clinical symptoms of osteoarthritis, Nat. Rev. Rheumatol. 6 (11) (2010) 625–635.
[86] M.B. Goldring, F. Berenbaum, The regulation of chondrocyte function by proinflammatory mediators: prostaglandins and nitric oxide, Clin. Orthop. Relat. Res. 427 (Suppl) (2004) S37–S46.
[87] N. Sofat, Analysing the role of endogenous matrix molecules in the development of osteoarthritis, Int. J. Exp. Pathol. 90 (5) (2009) 463–479.
[88] T. Hayashi, E. Abe, H.E. Jasin, Fibronectin synthesis in superficial and deep layers of normal articular cartilage, Arthritis Rheum. 39 (4) (1996) 567–573.
[89] C.M. Thomas, R. Murray, M. Sharif, Chondrocyte apoptosis determined by caspase-3 expression varies with fibronectin distribution in equine articular cartilage, Int. J. Rheum. Dis. 14 (3) (2011) 290–297.
[90] L. Lourido, V. Calamia, J. Mateos, P. Fernández-Puente, J. Fernández-Tajes, F.J. Blanco, et al., Quantitative proteomic profiling of human articular cartilage degradation in osteoarthritis, J. Proteome Res. 13 (12) (2014) 6096–6106.
[91] A.L. Clutterbuck, J.R. Smith, D. Allaway, P. Harris, S. Liddell, A. Mobasheri, High throughput proteomic analysis of the secretome in an explant model of articular cartilage inflammation, J. Proteome 74 (5) (2011) 704–715.
[92] J. Mateos, L. Lourido, P. Fernández-Puente, V. Calamia, C. Fernández-López, N. Oreiro, et al., Differential protein profiling of synovial fluid from rheumatoid arthritis and osteoarthritis patients using LC-MALDI TOF/TOF, J. Proteome 75 (10) (2012) 2869–2878.
[93] L. Balakrishnan, R.S. Nirujogi, S. Ahmad, M. Bhattacharjee, S.S. Manda, S. Renuse, et al., Proteomic analysis of human osteoarthritis synovial fluid, Clin. Proteomics 11 (1) (2014) 6.
[94] P. Fernández-Puente, J. Mateos, C. Fernández-Costa, N. Oreiro, C. Fernández-López, C. Ruiz-Romero, et al., Identification of a panel of novel serum osteoarthritis biomarkers, J. Proteome Res. 10 (11) (2011) 5095–5101.
[95] G. Morozzi, M. Fabbroni, F. Bellisai, G. Pucci, M. Galeazzi, Cartilage oligomeric matrix protein level in rheumatic diseases: potential use as a marker for measuring articular cartilage damage and/or the therapeutic efficacy of treatments, Ann. N. Y. Acad. Sci. 1108 (2007) 398–407.
[96] K. Misumi, M. Tagami, T. Kamimura, D. Miyakoshi, I.E. Helal, K. Arai, et al., Urine cartilage oligomeric matrix protein (COMP) measurement is useful in discriminating the osteoarthritic thoroughbreds, Osteoarthr. Cartil. 14 (11) (2006) 1174–1180.
[97] D. Ikeda, H. Ageta, K. Tsuchida, H. Yamada, iTRAQ-based proteomics reveals novel biomarkers of osteoarthritis, Biomarkers 18 (7) (2013) 565–572.
[98] J. Petzold, R. Casadonte, M. Otto, M. Kriegsmann, M. Granrath, A. Baltzer, et al., MALDI mass spectrometry of the meniscus. Objectification of morphological findings, Z. Rheumatol. 74 (5) (2015) 438–446.
[99] N. Georgi, B. Cillero-Pastor, G.B. Eijkel, P.C. Periyasamy, A. Kiss, C. van Blitterswijk, et al., Differentiation of mesenchymal stem cells under hypoxia and normoxia: lipid profiles revealed by time-of-flight secondary ion mass spectrometry and multivariate analysis, Anal. Chem. 87 (7) (2015) 3981–3988.
[100] M.T. Briggs, J.S. Kuliwaba, D. Muratovic, A.V. Everest-Dass, N.H. Packer, D.M. Findlay, et al., MALDI mass spectrometry imaging of *N*-glycans on tibial cartilage and subchondral bone proteins in knee osteoarthritis, Proteomics 16 (11–12) (2016) 1736–1741.
[101] A. Henss, M. Rohnke, T. El Khassawna, P. Govindarajan, G. Schlewitz, C. Heiss, et al., Applicability of ToF-SIMS for monitoring compositional changes in bone in a long-term animal model, J. R. Soc. Interface 10 (86) (2013) 20130332.
[102] J. Kokesch-Himmelreich, M. Schumacher, M. Rohnke, M. Gelinsky, J. Janek, ToF-SIMS analysis of osteoblast-like cells and their mineralized extracellular matrix on strontium enriched bone cements, Biointerphases 8 (1) (2013) 17.
[103] K. Schaepe, J. Kokesch-Himmelreich, M. Rohnke, A.S. Wagner, T. Schaaf, S. Wenisch, et al., Assessment of different sample preparation routes for mass spectrometric monitoring and imaging of lipids in bone cells via ToF-SIMS, Biointerphases 10 (1) (2015) 019016.
[104] P. Malmberg, H. Nygren, Methods for the analysis of the composition of bone tissue, with a focus on imaging mass spectrometry (TOF-SIMS), Proteomics 8 (18) (2008) 3755–3762.
[105] A. Henss, A. Hild, M. Rohnke, S. Wenisch, J. Janek, Time of flight secondary ion mass spectrometry of bone-impact of sample preparation and measurement conditions, Biointerphases 11 (2) (2015) 02A302.
[106] C.T. Chou, Binding of rheumatoid and lupus synovial fluids and sera-derived human IgG rheumatoid factor to degalactosylated IgG, Arch. Med. Res. 33 (6) (2002) 541–544.
[107] T. Matsuhashi, N. Iwasaki, H. Nakagawa, M. Hato, M. Kurogochi, T. Majima, et al., Alteration of *N*-glycans related to articular cartilage deterioration after anterior cruciate ligament transection in rabbits, Osteoarthr. Cartil. 16 (7) (2008) 772–778.
[108] A. Urita, T. Matsuhashi, T. Onodera, H. Nakagawa, M. Hato, M. Amano, et al., Alterations of high-mannose type *N*-glycosylation in human and mouse osteoarthritis cartilage, Arthritis Rheum. 63 (11) (2011) 3428–3438.
[109] C.R. Scanzello, Pathologic and pathogenic processes in osteoarthritis: the effects of synovitis, HSS J. 8 (1) (2012) 20–22.
[110] J. Bondeson, A.B. Blom, S. Wainwright, C. Hughes, B. Caterson, W.B. van den Berg, The role of synovial macrophages and macrophage-produced mediators in driving inflammatory and destructive responses in osteoarthritis, Arthritis Rheum. 62 (3) (2010) 647–657.
[111] E. Berntorp, A.D. Shapiro, Modern haemophilia care, Lancet 379 (9824) (2012) 1447–1456.
[112] E.C. Rodriguez-Merchan, Cartilage damage in the haemophilic joints: pathophysiology, diagnosis and management, Blood Coagul. Fibrinolysis 23 (3) (2012) 179–183.
[113] G. Roosendaal, F.P. Lafeber, Blood-induced joint damage in hemophilia, Semin. Thromb. Hemost. 29 (1) (2003) 37–42.
[114] G. Roosendaal, F.P. Lafeber, Pathogenesis of haemophilic arthropathy, Haemophilia 12 (Suppl. 3) (2006) 117–121.
[115] L.A. Valentino, Blood-induced joint disease: the pathophysiology of hemophilic arthropathy, J. Thromb. Haemost. 8 (9) (2010) 1895–1902.
[116] N.W. Jansen, G. Roosendaal, B. Lundin, L. Heijnen, E. Mauser-Bunschoten, J.W. Bijlsma, et al., The combination of the biomarkers urinary C-terminal telopeptide of type II collagen, serum cartilage oligomeric matrix protein, and serum chondroitin sulfate 846 reflects cartilage damage in hemophilic arthropathy, Arthritis Rheum. 60 (1) (2009) 290–298.
[117] G. Gerstner, M.L. Damiano, A. Tom, C. Worman, W. Schultz, M. Recht, et al., Prevalence and risk factors associated with decreased bone mineral density in patients with haemophilia, Haemophilia 15 (2) (2009) 559–565.
[118] C. Pauli, S.P. Grogan, S. Patil, S. Otsuki, A. Hasegawa, J. Koziol, et al., Macroscopic and histopathologic analysis of human knee menisci in aging and osteoarthritis, Osteoarthr. Cartil. 19 (9) (2011) 1132–1141.
[119] M.B. Goldring, K. Tsuchimochi, K. Ijiri, The control of chondrogenesis, J. Cell. Biochem. 97 (1) (2006) 33–44.
[120] F.J. Blanco, C. Ruiz-Romero, New targets for disease modifying osteoarthritis drugs: chondrogenesis and Runx1, Ann. Rheum. Dis. 72 (5) (2013) 631–634.
[121] S. Maddah, J. Mahdizadeh, Association of metabolic syndrome and its components with knee osteoarthritis, Acta Med. Iran. 53 (12) (2015) 743–748.
[122] W. Zhang, G. Sun, D. Aitken, S. Likhodii, M. Liu, G. Martin, et al., Lysophosphatidylcholines to phosphatidylcholines ratio predicts advanced knee osteoarthritis, Rheumatology (Oxford) 55 (9) (2016) 1566–1574.
[123] F. Sasazawa, T. Onodera, T. Yamashita, N. Seito, Y. Tsukuda, N. Fujitani, et al., Depletion of gangliosides enhances cartilage degradation in mice, Osteoarthr. Cartil. 22 (2) (2014) 313–322.
[124] D. Touboul, A. Brunelle, TOF-SIMS imaging of lipids on rat brain sections, Methods Mol. Biol. 1203 (2015) 21–27.
[125] M.A. Robinson, D.J. Graham, F. Morrish, D. Hockenbery, L.J. Gamble, Lipid analysis of eight human breast cancer cell lines with ToF-SIMS, Biointerphases 11 (2) (2016) 02A303.
[126] J.M. Castro-Perez, J. Kamphorst, J. DeGroot, F. Lafeber, J. Goshawk, K. Yu, et al., Comprehensive LC-MS E lipidomic analysis using a shotgun approach and its application to biomarker detection and identification in osteoarthritis patients, J. Proteome Res. 9 (5) (2010) 2377–2389.
[127] K.W. Frommer, A. Schäffler, S. Rehart, A. Lehr, U. Müller-Ladner, E. Neumann, Free fatty acids: potential proinflammatory mediators in rheumatic diseases, Ann. Rheum. Dis. 74 (1) (2015) 303–310.
[128] Q. Zhang, H. Li, Z. Zhang, F. Yang, J. Chen, Serum metabolites as potential biomarkers for diagnosis of knee osteoarthritis, Dis. Markers 2015 (2015) 684794.
[129] H. Miao, L. Chen, L. Hao, X. Zhang, Y. Chen, Z. Ruan, et al., Stearic acid induces proinflammatory cytokine production partly through activation of lactate-HIF1α pathway in chondrocytes, Sci. Rep. 5 (2015) 13092.
[130] O. Alvarez-Garcia, N.H. Rogers, R.G. Smith, M.K. Lotz, Palmitate has proapoptotic and proinflammatory effects on articular cartilage and synergizes with interleukin-1, Arthritis Rheum. 66 (7) (2014) 1779–1788.
[131] P. Roschger, B. Misof, E. Paschalis, P. Fratzl, K. Klaushofer, Changes in the degree of mineralization with osteoporosis and its treatment, Curr. Osteoporos. Rep. 12 (3) (2014) 338–350.

[132] D.G. Yu, S.B. Nie, F.X. Liu, C.L. Wu, B. Tian, W.G. Wang, et al., Dynamic alterations in microarchitecture, mineralization and mechanical property of subchondral bone in rat medial meniscal tear model of osteoarthritis, Chin. Med. J. 128 (21) (2015) 2879–2886.
[133] A.M. Costa, S.H. Lemos-Marini, M.T. Baptista, A.M. Morcillo, A.T. Maciel-Guerra, G. Guerra, Bone mineralization in turner syndrome: a transverse study of the determinant factors in 58 patients, J. Bone Miner. Metab. 20 (5) (2002) 294–297.
[134] A.C. Andrade, J. Baron, S.C. Manolagas, N.J. Shaw, G.A. Rappold, M.D. Donaldson, et al., Hormones and genes of importance in bone physiology and their influence on bone mineralization and growth in turner syndrome, Horm. Res. Paediatr. 73 (3) (2010) 161–165.
[135] N. Fratzl-Zelman, B.M. Misof, K. Klaushofer, P. Roschger, Bone mass and mineralization in osteogenesis imperfecta, Wien. Med. Wochenschr. 165 (13–14) (2015) 271–277.
[136] NIH Consensus Development Panel on Osteoporosis Prevention, Diagnosis, and therapy, March 7–29, 2000: highlights of the conference, South. Med. J. 94 (6) (2001) 569–573.
[137] P. Malmberg, U. Bexell, C. Eriksson, H. Nygren, K. Richter, Analysis of bone minerals by time-of-flight secondary ion mass spectrometry: a comparative study using monoatomic and cluster ions sources, Rapid Commun. Mass Spectrom. 21 (5) (2007) 745–749.
[138] P.J. Marie, P. Ammann, G. Boivin, C. Rey, Mechanisms of action and therapeutic potential of strontium in bone, Calcif. Tissue Int. 69 (3) (2001) 121–129.